Performance comparison between piezoelectric and CMUT probes in measuring the backscattering coefficient

Lenin Chinchilla, Emilie Franceschini, Alessandro S Savoia

2019 INTERNATIONAL CONGRESS ON ULTRASONICS
BRUGES, BELGIUM, 3-6 SEPT 2019

Performance comparison between piezoelectric and CMUT probes in measuring the backscattering coefficient

Lenin Chinchilla[1,2], **Emilie Franceschini**[1], **Alessandro S. Savoia**[2]

[1]*LMA UMR 7031, Aix-Marseille University, 4 impasse Nikola Tesla, 13453 Marseille Cedex 13, France*
[2]*Department of Engineering, Roma Tre University, via della Vasca Navale 84, 00146 Rome, Italy*

Abstract
In the field of quantitative ultrasound (QUS), evaluation of tissue-anisotropy plays a key role in the description of the tissue microstructure. Several studies have been conducted to parameterize the tissue-anisotropy by measuring the angular dependence of the backscatter-coefficient. The seminal works were carried out by using a single element transducer, and more recent ones using ultrasound linear array probes. However, the performance of the probe imposes a limit for the maximal angle to which measurements can be performed. For instance, the element directivity and cross-talk are probe features that affect the probe performance, independently of the imaging strategy used, either the focused beam steering or the plane wave imaging. In this work we present a comparative analysis between a Capacitive Micromachined Ultrasonic Transducer (CMUT) probe and a commercial piezoelectric probe, in which the BSC is measured using the focused beam steering imaging strategy on an isotropic tissue-mimicking phantom along different beam steering angles. The results show that the CMUT probe exhibits better performance than the piezoelectric probe in terms of larger usable bandwidth and wider angular range in which the BSC measurements can be performed.

Keywords
Backscatter-coefficient, anisotropic, piezoelectric probe, CMUT probe, focused beam steering

I. Introduction
Quantitative ultrasound (QUS) techniques based on the parameterization of the backscatter coefficient (BSC) [1,2] are now routinely used in tissue characterization. A scattering model is fit to the estimated BSC and the fit parameters can provide a meaningful description of the tissue microstructure (i.e., scatterer size, shape, scattering properties and spatial organization). Most of QUS approaches assume that the tissue under characterization is homogeneous and isotropic [3,4]. However, some biological tissues, such as flowing aggregating blood [5,6], bicep muscles [7] and myocardium [8] show angle-dependent acoustic properties (BSC and/or attenuation coefficient). Garcia-Duitama [6] and Guerrero [7] recently proposed anisotropic QUS parameters by using reference phantom method to compensate for the electromechanical system response when performing plane wave imaging beamforming or conventional focused beam steering with a linear array. One of the limitations remains the maximum angle to which the BSC measurements can be performed, which is defined by the probe steering capability that depends on element directivity (array design) and cross-talk noise (technology). In this work, a performance comparison is carried out between a Capacitive Micromachined Ultrasonic Transducer (CMUT) probe and a piezoelectric probe to measure the BSC from an isotropic tissue-mimicking phantom using the focused beam steering imaging strategy. Then the spectra and BSC results for different beam steering angles are compared.

II. Methodology
II.1 Tissue-mimicking phantoms
Two tissue-mimicking phantoms consisting of embedded polyamide particles in an agar-agar gel background were used in this study. The tissue-mimicking phantom to be characterized(referred as the sample) contains 11 µm -diameter polyamide particles (orgasol 2001 EXD NAT 1, Arkema, France) with longitudinal speed of sound $c_s = 1505.6 m/s$ and power-law

attenuation coefficient $\alpha_s = 0.0155\text{dB/cm}/MHz^b$ with *b*=1.57, whereas the reference tissue-mimicking phantom contains 6 µm -diameter polyamide particles (orgasol 2001 UD NAT 1, Arkema, France) with longitudinal speed of sound $c_{ref} = 1504.5m/s$ and power-law attenuation coefficient $\alpha_{ref} = 0.0214\text{dB/cm}/MHz^b$ with *b*=1.34.

II.2 Experiments

The ultrasound open scanner ULA-OP [9] was used to drive the ultrasound probe and collect ultrasound radio-frequency (RF) data. The probe was excited with a one-cycle sinusoidal burst at 10 MHz. In transmission, the beam steering angles were varied from -30º to 30º in steps of 5º, by keeping the focusing depth at 15 mm and using an aperture of 32 elements. In reception, dynamic receive beamforming was performed to each transmitted beam steering, using an aperture of 64 elements and a *f-number* of 1.18. The probe was placed at 10 cm from the tissue-mimicking phantom interface and raw RF data for all the beam steering angles were acquired from 10 uncorrelated frames of RF echo signals for both tissue-mimicking phantoms. The experiments were carried out by using two linear probes, the piezoelectric probe LA435 (ESAOTE, Florence, Italy) (*fc*=11 MHz, pitch=0.2 mm), and the HF3 CMUT [10] prototype probe (*fc* =9.5 MHz, pitch=0.2 mm). The raw RF data were then post-processed by using the MATLAB software.

II.2 Spectral parameter estimation

For each acquired B-mode frame, a region-of-interest (ROI) was selected around the focal zone. The ROIs corresponded to 100 echo lines laterally and 27 wavelengths axially, gated with a rectangular window. Each ROI provides an estimated power spectrum, which is computed by averaging the squared fast Fourier transform of all the echo-lines in the ROI. Then the power spectra from the ROIs is averaged to obtain the spectrum used to compute the BSC. The BSC was then estimated using the reference phantom method [11], for which the power spectra of the sample and of the reference phantom, $S_s^2(\theta, f)$ and $S_{ref}^2(\theta, f)$, are estimated from backscattered data obtained using the same imaging settings to compensate the system-dependent effects. The BSC is estimated as

$$BSC_s(\theta, f) = BSC_{ref}(f)\frac{S_s^2(\theta,f)}{S_{ref}^2(\theta,f)}e^{4z_d(\alpha_s(f)-\alpha_{ref}(f))}, \quad (1)$$

where θ is the transmitted and received beam steering angle, and z_d is the depth of the ROI. The last term in Eq. (1), i.e. the exponential function, compensates for attenuation effects. The $BSC_{ref}(f)$ is the known BSC of the reference given by Eq. (2) in Franceschini *et.al.* [12] using the Faran model [13].

Finally, the integrated backscatter coefficient (iBSC) was computed as

$$iBSC(\theta) = \frac{1}{BW}\int_{BW} 10log_{10}(BSC(\theta, f))df, \quad (2)$$

where *BW* corresponds to the analyzed bandwidth.

III. Results and discussion

Figure 1 shows the power spectra of the sample using both piezoelectric and CMUT probes for different beam steering angles. The piezoelectric probe has 73% -6dB fractional bandwidth centered at *fc*=11 MHz. The CMUT probe shows a broader bandwidth, i.e., 84% bandwidth centered at *fc*=9.5 MHz, with respect to the piezoelectric probe, as demonstrated in different studies [10]. In addition, the power spectra from the CMUT probe are symmetrical with respect to the center frequency *fc*, for all the considered beam steering angle, whereas, the power spectra from the piezoelectric probe exhibit distortion that increases as the beam steering angle increases. This frequency distortion may come from 1) the high ultrasonic pressure produced by the piezoelectric probe (in comparison with the CMUT probe) that produces nonlinear distortion of the ultrasound signal, and/or 2) the alteration of the beam pattern as

reported by Ramalli *et al.* [14]. When using piezoelectric probes, Ramalli *et al.* [14] demonstrated that the cross-talk between neighbor elements produce beam deformation, accompanied by the reduced beam steering angle. Further studies need to be conducted to deeply investigate the origin of the observed frequency distortion.

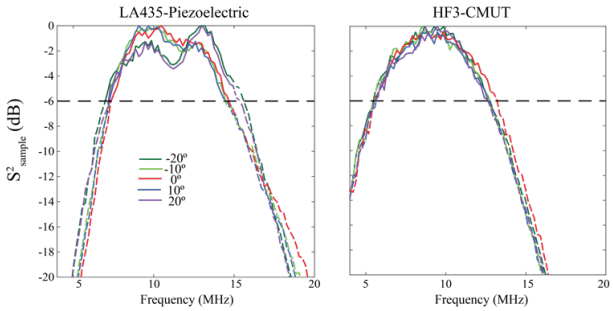

Figure 1. Power spectra for different beam steering angles for both piezoelectric and CMUT probes. The dashed represents the -6dB bandwidth.

Figure 2 presents the BSC obtained from both piezoelectric and CMUT probes for different beam steering angles. For both probes, there is a good agreement between the BSC curves whatever the studied beam steering angles. When considering the piezoelectric probe, no impact due to the power spectra distortion observed in Fig. 1 is observed on the BSC curves. These results suggest that the reference phantom technique allows to compensate for the frequency distortion. However, the acoustic properties (sound speed, attenuation, nonlinear *B/A* parameter) from the reference and sample phantoms are very similar. We should verify that the compensation for the frequency distortion is still efficient when the properties of the reference phantom (especially the nonlinear *B/A* parameter) differs from the sample.

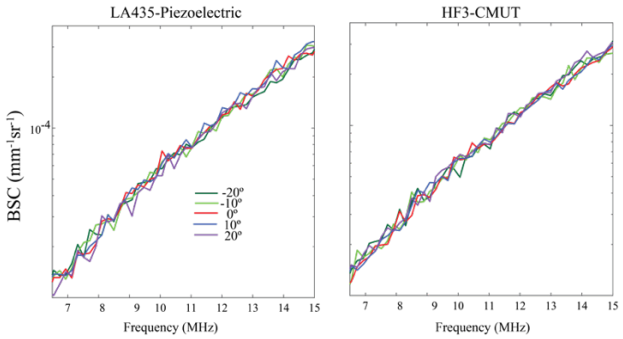

Figure 2. Frequency-dependent BSCs for different beam steering angles for both piezoelectric and CMUT probes.

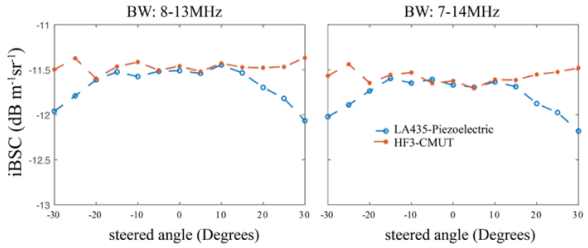

Figure 3. The integrated backscatter coefficient versus beam steering angles for two different bandwidths 8-13MHz and 7-14MHz.

Figure 3 presents the iBSC as a function of the beam steering angle for two different bandwidths: 8-13 MHz and 7-14 MHz. The maximal difference in the iBSC is about 0.5 dB. This result agrees well with the averaged normalized backscattered power difference (mBSPD≈0.41 dB) measured from an isotropic tissue-mimicking phantom (see Guerrero *et al.*[7], Fig. 8). Given that measurements were taken from an isotropic phantom, the same value for all the beam steering angles is expected in the iBSC. Similar iBSC values were obtained

for all the beam steering angles ranging from -30° to 30° (with difference less than 0.15 dB) for the CMUT probe and for the beam steering angles ranging from -15° and 15° (with difference less than 0.6 dB) for the piezoelectric probe.

IV. Conclusion

We have compared the performance of CMUT and piezoelectric probes to measure the BSC from an isotropic tissue mimicking phantom using the beam steering approach. For beam steering angles ranging from -15º to 15º, both CMUT and piezoelectric probes present similar iBSC values for the two analyzed bandwidths 8-13 MHz and 7-14 MHz. For wider steering angles, the iBSC was more accurately estimated with the CMUT probe. Moreover, the CMUT probe presents a wider usable bandwidth in comparison with the piezoelectric probe. The results of this analysis allows us to conclude that the typical features of CMUT probes, i.e. large bandwidth and low crosstalk, offer advantages over piezoelectric probes in measuring the BSC, which can be exploited either to perform conventional on-axis BSC measurements, as well as BSC measurements in wide angular ranges.

Acknowledgements

This work was supported by the financial support of the French National Research Agency (Grant No. ANR-15-CE19-0017), the Labex MEC (Grant No. ANR-10-LABX-0092) and the Colombian department of Science and technology COLCIENCIAS.

References

[1] R. de Monchy, J. Rouyer, F. Destrempes, B. Chayer, G. Cloutier, E. Franceschini, *Estimation of polydispersity in aggregating red blood cells by quantitative ultrasound backscatter analysis, J. Acoust. Soc. Amer.*, 143(4) **2018**, 2207-2216

[2] P. Muleki-Seya, R. Guillermin, J. Guglielmi, J. Chen, T. Pourcher, E. Konofagou, E. Franceschini, *High frequency quantitative ultrasound spectroscopy of excised canine livers and mouse tumors using the structure factor model*, *IEEE Trans. on Ultrason.,* Ferroelect. Freq. Contr., 63(9) **2016**, 1335-1350

[3] E.L. Madsen, M.F. Insana, J.A. Zagzebski, *Method of data reduction for accurate determination of acoustic backscatter coefficients*, *J. Acoust. Soc. Amer., 76*(3) **1984**, 913-923.

[4] S.C. Lin,E. Heba, T. Wolfson, B. Ang, A. Gamst, A. Han, ..., R. Loomba, *Noninvasive diagnosis of nonalcoholic fatty liver disease and quantification of liver fat using a new quantitative ultrasound technique*, *Clinical Gastroenterology and Hepatology*, *13*(7) **2015**, 1337-1345.

[5] C. Guilbert, F. Yu, G. Cloutier, *11C-6 New Observations on the Anisotropy of Ultrasound Blood Backscatter as a Function of Frequency and Shear Rate, Proc. IEEE IUS*, **2007,** 1013-1016

[6] J. Garcia-Duitama, B. Chayer, A. Han, D. Garcia, M.L. Oelze, G. Cloutier, (2015), *Experimental application of ultrafast imaging to spectral tissue characterization*. *Ultrasound in Med. & Biol.*, 41(9) **2015**, 2506-2519.

[7] Q.W. Guerrero, I.M. Rosado-Mendez, L.C. Drehfal, H. Feltovich, T.J. Hal, *Quantifying backscatter anisotropy using the reference phantom method*, *IEEE UFFC*, *64*(7) **2017**, 1063-1077.

[8] M. Yang, T.M. Krueger, J.G. Miller, M.R. Holland, *Characterization of anisotropic myocardial backscatter using spectral slope, intercept and midband fit parameters*, *Ultrason. imaging*, *29*(2) **2007**, 122-134.

[9] P. Tortoli, L. Bassi, E. Boni, A. Dallai, F. Guidi and S. Ricci, *ULA-OP: an advanced open platform for ultrasound research*, *IEEE UFFC,* 56(10), **2009,** 2207-16.

[10] A.S. Savoia, G. Caliano, M. Pappalardo, *A CMUT probe for medical ultrasonography: from microfabrication to system integration*, *IEEE UFFC,* 59(6) **2012,**1127-38.

[11] L.X Yao, J.A. Zagzebski, E.L. Madsen, *Backscatter coefficient measurements using a reference phantom to extract depth-dependent instrumentation factors, Ultrason. Imaging,* 12(1) **2015,** 58-70

[12] E. Franceschini, R. Guillermin, *Experimental assessment of four ultrasound scattering models for characterizing concentrated tissue-mimicking phantoms*, *J. Acoust. Soc. Amer.,* 132(6) **2012**, 3735-3747

[13] J.J Faran Jr, *Sound scattering by solid cylinders and spheres*, *J. Acoust. Soc. Amer.,* 23(4) **1951**, 405-418.

[14] A. Ramalli, P. Tortoli, A. S. Savoia, G. Caliano, *Improved array beam steering by compensation of inter-element cross-talk*, *Proc. IEEE IUS*, **2015**, 1-4